An analytical model for predicting airfoil self-noise using wall-pressure statistics

By M. Roger †, S. Moreau ‡ AND M. Wang

1. Motivation and objectives

Broadband self-noise or trailing-edge noise is due to the scattering of boundary-layer vortical disturbances into acoustic waves at the trailing edge of an airfoil. As the only airfoil noise contribution in a homogeneous stationary flow, it is a matter of primary interest when addressing the problem of the noise generated by fans, wind turbines and high-lift devices. Simple aeroacoustic prediction tools dedicated to trailing-edge noise, that could be integrated in a design cycle, are a current need for manufacturers. In the context of industrial applications, a minimum degree of relevance is required, but the fine details of the scattering process are not expected to be reproduced exactly. A consistent model only has to provide reliable A-weighted levels, which means a realistic distribution of noise intensity with both frequency and angle of radiation, accurate enough for a definition in terms of decibels. Such tools can be deduced from analytical models and could be used in conjunction with incompressible flow computations, according to the acoustic analogy as stated by Ffowcs Williams & Hawkings (1969).

As a result of the scattering of a boundary layer turbulent flow, self noise can be related either to the vortical, hydrodynamic velocity field around the trailing-edge or to the induced hydrodynamic pressure field on the airfoil surface. The first approach, based on the velocity field, is outlined by Ffowcs Williams & Hall (1970) and was applied by Wang & Moin (2000) using large-eddy simulation results as input. The second approach, based on the induced wall pressure, has been developed and applied, for instance by Brooks & Hodgson (1981) and Amiet (1976), but rarely addresses the connection with computational results. It is supported by experimental evidence, as pointed out by Brooks, Marcolini & Pope (1989) and Roger & Moreau (2002).

The present work is an extension of Amiet's original formulation of trailing-edge noise based on fully analytical derivations. A back-scattering, leading edge correction is developed, yielding a modified chordwise distribution of the acoustic sources induced by the scattering mechanism. Furthermore, a three-dimensional extension is provided. The full solution has the advantage of accounting for all the effects of a finite chord length. The study is aimed at predicting airfoil self noise from wall pressure fluctuations computed by incompressible LES. In that sense, the present formulation is an alternative to the one proposed by Ffowcs Williams & Hall (1970), and has the advantage that both the actual chord length and any subsonic motion of the surrounding fluid are accounted for.

† Ecole Centrale de Lyon (ECL), France
‡ VALEO Motors and Actuators, France

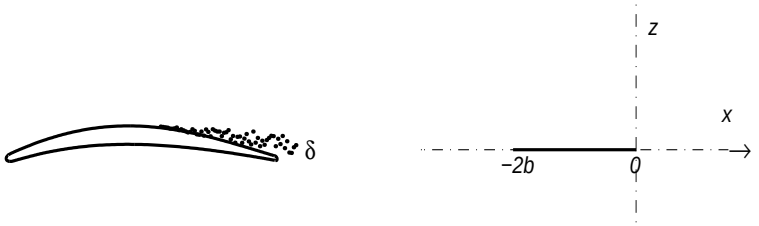

FIGURE 1. Flat-plate model of an airfoil with moderate camber and thickness. The boundary layer vorticity (thickness δ) is represented by equivalent convected pressure fluctuations.

2. Results

2.1. *Far-field power spectral density*

In the present analytical model, the airfoil is reduced to a flat plate with zero thickness and angle of attack, with a chord length $c = 2b$ and a span L. The space is described by the streamwise coordinate x, the spanwise coordinate y and the normal z coordinate. The trailing edge is at $x = 0$ (figure 1). The fluid is moving uniformly with velocity U along the chordwise direction $x > 0$. The corresponding Mach number $M = U/c_0$ with c_0 the speed of sound is assumed subsonic. The acoustic wavenumber $k = \omega/c_0$ is related to the convective wavenumber $K = \omega/U$ by the relationship $k = KM$.

The power spectral density of the far field sound pressure radiated from the airfoil due to the lift fluctuations induced by trailing-edge scattering can be expressed in the following way, extending the results of Amiet (1975):

$$S_{pp}(\vec{x},\omega) = \left(\frac{\omega\, z\, L\, b}{2\,\pi\, c_0 S_0^2}\right)^2 \frac{1}{b} \int_{-\infty}^{\infty} \Pi_0(\frac{\omega}{U_c}, K_2)\, \mathrm{sinc}^2\left\{\frac{L}{2b}(\bar{K}_2 - \bar{k}\frac{y}{S_0})\right\} \left| I(\frac{\bar{\omega}}{U_c}, \bar{K}_2)\right|^2 d\bar{K}_2 \tag{2.1}$$

with:

$$\mathrm{sinc}\,(t) = \frac{\sin(t)}{t}$$

In this formula, I is the radiation integral associated with a two-dimensional Fourier component of the incident hydrodynamic wall pressure field, with hydrodynamic wavenumbers K_1 and K_2 respectively in the streamwise and spanwise directions. This incident field is assumed frozen when convected past the trailing edge, which selects the value of the streamwise wavenumber $K_1 = \omega/U_c$. U_c is the convection speed, related to U by the factor $\alpha = U/U_c > 1$. $S_0 = \sqrt{x^2 + \beta^2(y^2 + z^2)}$ is the corrected distance to the far field point $\vec{x}$, with $\beta^2 = 1 - M^2$, and $(\bar{\cdot})$ stands for quantities made nondimensional by multiplying by b. Π_0 is the energy of the incident wall pressure fluctuations at angular frequency ω for a given spanwise wavenumber. It is deduced from the full cross spectral density function of the incident wall pressure $\Pi(K_1, K_2, \omega)$:

$$\Pi_0(\frac{\omega}{U_c}, K_2) \;=\; \int_{-\infty}^{\infty} \Pi(K_1, K_2, \omega)\, dK_1 \tag{2.2}$$

In (2.2), Π represents a huge amount of information hardly tractable in experiments. Only accurate numerical methods, such as Direct Numerical Simulation or Large Eddy Simulation, are able to provide the necessary data by explicitly computing the wall pressure fluctuations associated with most of the turbulent eddies carrying the energy

of the vortical flow. Yet the full statistics Π appears not to be necessary for the present acoustic formulation. Indeed let's introduce:

$$\Pi(K_1, K_2, \omega) \;=\; \frac{1}{4\,\pi^2} \int\int \Omega_{pp}(\eta_1, \eta_2, \omega)\, e^{i\,(K_1\eta_1 + K_2\eta_2)}\, d\eta_1\, d\eta_2 \tag{2.3}$$

where Ω_{pp} is the cross-spectral density between signals at two points on the airfoil with separations η_1 and η_2 in the streamwise and spanwise directions. Then let's define the functions A and B as in Singer (1996):

$$A(\eta_1, \omega) \;=\; \frac{\Omega_{pp}(\eta_1, 0, \omega)}{\Phi_{pp}(\omega)} \qquad B(\eta_2, \omega) \;=\; \frac{\Omega_{pp}(0, \eta_2, \omega)}{\Phi_{pp}(\omega)} \tag{2.4}$$

where Φ_{pp} is the wall pressure spectrum corresponding to the incident hydrodynamic fluctuations only, assumed statistically homogeneous in the trailing-edge area. Without any further assumption on the wall pressure statistics, equation (2.2) then becomes accounting for (2.3) and (2.4):

$$\Pi_0(\frac{\omega}{U_c}, K_2) \;=\; \int_{-\infty}^{\infty} \Pi(K_1, K_2, \omega)\, dK_1 \;=\; \frac{\Phi_{pp}}{2\,\pi} \int_{-\infty}^{\infty} B(\eta_2, \omega)\, e^{i\,K_2\,\eta_2}\, d\eta_2$$

The more tractable parameter in connection with model experiments is the wall pressure field coherence between two points on the airfoil surface:

$$\gamma^2(\eta_1, \eta_2, \omega) \;=\; \frac{|\Omega_{pp}(\eta_1, \eta_2, \omega)|^2}{\Phi_{pp}^2(\omega)}$$

Therefore, the coherence can be identified to the squared chordwise and spanwise correlation functions A and B, respectively, as the separation η_2 or η_1 is set to zero. If the following corrected correlation length $l_y(\omega)$ is introduced:

$$l_y(K_2, \omega) \;=\; \int_0^{\infty} \sqrt{\gamma^2(0, \eta_2, \omega)}\, \cos(K_2\eta_2)\, d\eta_2$$

a final expression can be derived for the energy of the incident wall pressure fluctuations at frequency ω for a given spanwise wavenumber:

$$\Pi_0(\frac{\omega}{U_c}, K_2) \;=\; \frac{1}{\pi}\, \Phi_{pp}(\omega)\, l_y(K_2, \omega) \tag{2.5}$$

Functions Φ_{pp} and l_y are the minimum informations about the wall pressure statistics, needed for acoustic calculations. They are easy to measure on a model airfoil by means of a set of wall pressure transducers, spanwise distributed at a short distance upstream of the trailing edge. Such transducers, when located beneath a fully turbulent boundary layer, measure a priori the full wall pressure field, including the acoustic contamination from the trailing-edge scattering. However the acoustic pressure is typically 20 decibels below the hydrodynamic pressure associated with the convected turbulence. Thus the measured pressure can be assimilated to the hydrodynamic pressure only in this case. This is confirmed by the values of the convection speed measured by Roger & Moreau

(2002). As a consequence, trailing-edge transducers provide the same information as that computed in incompressible LES.

2.2. *Radiation integral*

Calculating the distant sound field with (2.1) still requires the computation of the radiation integral $I(\bar{\omega}/U_c, \bar{K}_2)$, which holds for a unit gust of reduced wavenumber vector $(\bar{K}_1 = \bar{\omega}/U_c, \bar{K}_2)$, at angular frequency ω. This vector defines an incident hydrodynamic oblique gust of unit pressure:

$$P_0 \,=\, e^{-i\bar{K}_1 X}\, e^{-i\bar{K}_2 Y}$$

with $X = x/b$ and $Y = y/b$, leading to a three-dimensional scattering problem. The equation for the corresponding scattered pressure is:

$$\frac{\partial^2 p'}{\partial x^2} \,+\, \frac{\partial^2 p'}{\partial z^2} \,+\, \frac{\partial^2 p'}{\partial y^2} \,-\, \frac{1}{c_0^2}\left(\frac{\partial}{\partial t} \,+\, U\,\frac{\partial}{\partial x}\right)^2 p' \,=\, 0$$

together with the boundary condition of no cross-flow on the airfoil surface and the cancellation of P_0 in the wake according to the Kutta condition. The solution is sought in the form:

$$p'(x,y,z,t) \,=\, P(x,y,z)\, e^{i\,\omega\, t}$$

$$P(x,y,z) \,=\, p(x,z)\, e^{i(kM/\beta^2)x}\, e^{-i\,K_2\, y} \,=\, p(X,Z)\, e^{i\,M\bar{\mu}X}\, e^{-i\,\bar{K}_2 Y}$$

with $\bar{\mu} \,=\, \bar{K}M/\beta^2$. Introducing $Z = \beta z/b$, the equation becomes:

$$\frac{\partial^2 p}{\partial X^2} \,+\, \frac{\partial^2 p}{\partial Z^2} \,+\, \bar{\kappa}^2\, p \,=\, 0 \qquad \text{in which} \qquad \bar{\kappa}^2 \,=\, \bar{\mu}^2 \,-\, \frac{\bar{K}_2^2}{\beta^2} \tag{2.6}$$

with

$$\frac{\partial p}{\partial Z}\,(X,0) \,=\, 0 \qquad\qquad -2 < X < 0$$

$$p(X,0) \,=\, -e^{-i\,(\bar{K}_1 + M\bar{\mu})X} \qquad\qquad X > 0$$

Supercritical gusts, corresponding to positive values of $\bar{\kappa}^2$ (i.e. real $\bar{\kappa} = \sqrt{\bar{\mu}^2 \,-\, \bar{K}_2^2/\beta^2}$), thus a hyperbolic equation, are known to radiate efficiently, whereas subcritical gusts, for which $\bar{\kappa} = -i\,\kappa'$ is imaginary ($\kappa' = \sqrt{(\bar{K}_2^2/\beta^2) \,-\, \bar{\mu}^2}$), are less efficient. The differential equation for p has no exact solution but can be solved by successive iterations. The first iteration is performed by assuming that the airfoil extends towards infinity in the upstream direction instead of the leading edge location $X = -2$. A Schwarzschild's problem is obtained, whose basic solution is summarized in the appendix. This first solution has been derived by Amiet (1976) in the case of two-dimensional gusts. Later Amiet (1978) refined the solution to account for the radiation effect of the incident pressure. The corresponding scattered field must be corrected to behave properly upstream. This is made by adding a leading edge back-scattered field ensuring a zero total disturbance potential for $X < -2$. The correction is calculated assuming that the airfoil now extends

towards infinity in the downstream direction from the leading edge, which leads to another Schwarzschild's problem by a straightforward change of variables. The technique has been described by Amiet (1975) dealing with the similar problem of the noise generated when upstream turbulence impinges on the leading edge of an airfoil. Generally speaking, the Schwarzschild's solution holds for the pressure disturbance when applied at the trailing edge and for the velocity potential ϕ when applied at the leading edge, with:

$$-\frac{b}{\rho_0 U}\,P \;=\; \frac{\partial \phi}{\partial X} \;+\; i\,\bar{K}\,\phi$$

The new items with respect to the original papers are the additional leading edge back–scattering correction for trailing-edge noise and the extension to three-dimensional scattering, accounting for subcritical gusts. The Schwarzschild's iterative procedure provides the value of p on the airfoil surface, used to calculate the radiation integral I. Only the final results are given here.

I can be written as $I = I_1 + I_2$, where I_1 stands for the main scattering from the trailing edge and I_2 for the back–scattering from the leading edge.

The first term for a supercritical gust, already obtained by Amiet (1978) in the two-dimensional case, is given by:

$$I_1 \;=\; -\,\frac{e^{2iC}}{iC}\left\{(1+i)\,e^{-2\,i\,C}\,\sqrt{\frac{B}{B-C}}\,E^*[2(B-C)] \;-\; (1+i)E^*[2B]\right\} \tag{2.7}$$

with:

$$C \;=\; \bar{K}_1 - \bar{\mu}\left(\frac{x}{S_0} - M\right) \qquad \text{and} \qquad B \;=\; \bar{K}_1 + M\,\bar{\mu} + \bar{\kappa}$$

The correction term derived in the present work is:

$$I_2 \;=\; H\,\left(\left\{e^{4\,i\,\bar{\kappa}}\,\left[1 \;-\; (1+i)\,E^*(4\,\bar{\kappa})\right]\right\}^c \;-\; e^{2i\,D} \;+\; i\,[D + \bar{K} + M\,\bar{\mu} \;-\; \bar{\kappa}]\,G\right) \tag{2.8}$$

with

$$\begin{aligned} G \;=\; & (1+\epsilon)\,e^{i\,(2\bar{\kappa}+D)}\,\frac{\sin(D-2\,\bar{\kappa})}{D-2\,\bar{\kappa}} \;+\; (1-\epsilon)\,e^{i\,(-2\bar{\kappa}+D)}\,\frac{\sin(D+2\,\bar{\kappa})}{D+2\,\bar{\kappa}} \\ & + \frac{(1+\epsilon)(1-i)}{2(D-2\,\bar{\kappa})}\,e^{4\,i\,\bar{\kappa}}\,E^*(4\,\bar{\kappa}) \;-\; \frac{(1-\epsilon)(1+i)}{2(D+2\,\bar{\kappa})}\,e^{-4\,i\,\bar{\kappa}}\,E(4\,\bar{\kappa}) \\ & + \frac{e^{2\,i\,D}}{2}\,\sqrt{\frac{2\bar{\kappa}}{D}}\,E^*(2D)\,\left[\frac{(1+i)(1-\epsilon)}{D+2\bar{\kappa}} \;-\; \frac{(1-i)(1+\epsilon)}{D-2\bar{\kappa}}\right] \end{aligned}$$

and

$$D = \bar{\kappa} - \bar{\mu}\,x/S_0 \qquad H \;=\; \frac{(1+i)\,e^{-4\,i\,\bar{\kappa}}\,(1-\Theta^2)}{2\,\sqrt{\pi}\,(\alpha-1)\,\bar{K}\,\sqrt{B}} \qquad \epsilon \;=\; \frac{1}{\sqrt{1+1/(4\bar{\kappa})}}$$

$$\Theta \;=\; \sqrt{\frac{A_1}{A}} \qquad A_1 \;=\; \bar{K}_1 + M\bar{\mu} + \bar{\kappa} \qquad A \;=\; \bar{K} + M\bar{\mu} + \bar{\kappa}$$

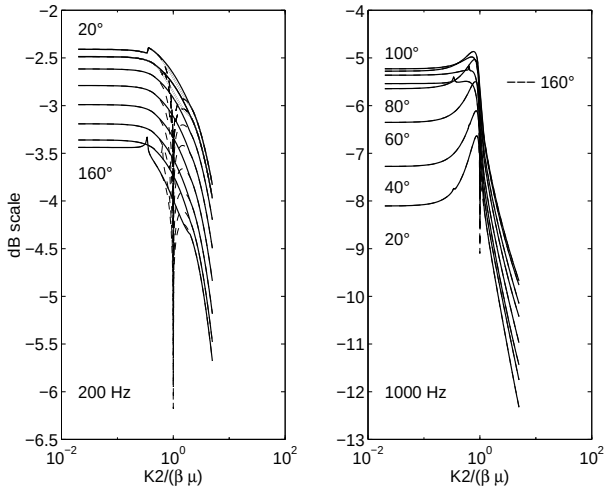

FIGURE 2. Profiles of the radiation integral $|I|$ in nondimensional variables, for radiation angles θ (in 20° increment) with respect to the flow direction in the mid-span plane. $M = 0.05$. - - - regularization off, — regularization on.

In both equations (2.7) and (2.8), the complex function E^* stands for a combination of Fresnels integrals C_2 and S_2 given in Abramowitz & Stegun (1970) and is defined as:

$$E^*(x) \,=\, \int_0^x \frac{e^{-it}}{\sqrt{2\pi t}}\, dt \,=\, C_2(x) \,-\, i\, S_2(x)$$

$\{\cdot\}^c$ stands for quantities whose imaginary part needs to be multiplied by the empirical corrective factor ϵ. The latter has been determined numerically to yield an analytical form for the back-scattering radiation integral.

Equivalent results have been derived for a subcritical gust, leading to the following expressions:

$$I_1 = -\frac{e^{2\,i\,C}}{i\,C}\left\{e^{-2\,i\,C}\,\sqrt{\frac{A_1'}{\bar{\mu}\,(\frac{x}{S_0}) - i\,\bar{\kappa'}}}\,\Phi^\circ\left(\sqrt{2i\,(\bar{\mu}\,(\frac{x}{S_0}) - i\,\bar{\kappa'})}\right) - \Phi^\circ\left(\sqrt{2i\,A_1'}\right)\right\} \quad (2.9)$$

and

$$I_2 = \frac{e^{-2\,i\,B}}{B}\,H'\left\{A'\left(e^{2iB}\left[1 - \mathrm{erf}(\sqrt{4\bar{\kappa'}})\right] - 1\right) + \sqrt{2\bar{\kappa'}}\left(\bar{K} + (M - \frac{x}{S_0})\bar{\mu}\right)\frac{\Phi^\circ(\sqrt{-2i\bar{B}})}{\sqrt{-i\bar{B}}}\right\} \quad (2.10)$$

with

$$H' \,=\, \frac{(1+i)\,(1-\Theta'^2)}{2\,\sqrt{\pi}\,(\alpha-1)\,\bar{K}\,\sqrt{A_1'}} \qquad \Theta' \,=\, \sqrt{\frac{A_1'}{A'}}$$

$$A_1' \,=\, \bar{K}_1 + M\bar{\mu} - i\,\bar{\kappa'} \qquad A' \,=\, \bar{K} + M\bar{\mu} - i\,\bar{\kappa'}$$

In both equations (2.9) and (2.10), a new complex function Φ° is introduced that is

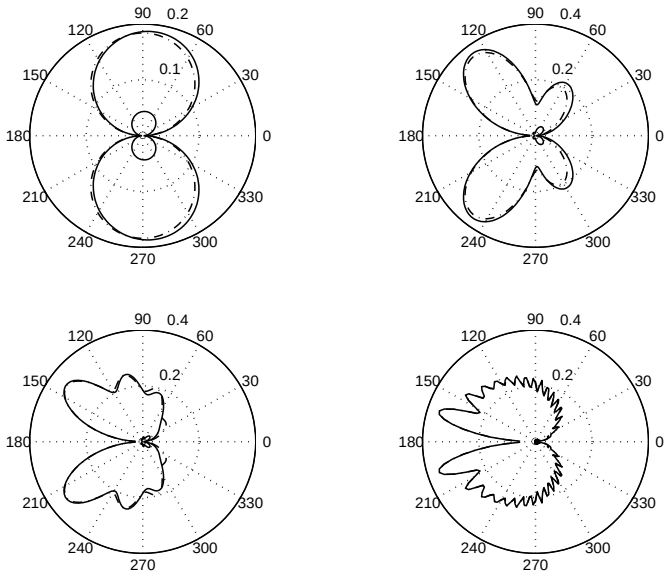

FIGURE 3. Directivity patterns for parallel gusts. From left to right and top to bottom: $kc = 1, 5, 10, 50$ for comparison with Howe (2001). $M = 0.05$, $\bar{K}_2 = 0$. — full solution, -.- main term, — back-scattering (small lobes at center).

related to the complex E^* by:

$$\Phi^\circ(Z) \,=\, \frac{1}{\sqrt{\pi}} \int_0^{Z^2} \frac{e^{-z}}{\sqrt{z}}\, dz \qquad \text{and} \qquad \Phi^\circ(\sqrt{i\,x}) \,=\, \sqrt{2}\, e^{i\,\pi/4}\, E^*(x)$$

Sample non-dimensional K_2-profiles of I for an observer in the mid-span plane ($y = 0$) are given in figure 2. A regularization procedure has been applied to smooth out the sharp cuts in the profiles between the supercritical and subcritical expressions understood as asymptotic solutions. The cuts are due to the breakdown of the analytical solution as the frequency parameter $\bar{\kappa}$ or $\bar{\kappa}'$ becomes exactly zero. The procedure is achieved by matching linearly the values of the derivative $\partial I/\partial K_2$ from both sides of the cuts and then re-calculating the profile. Subcritical gusts, for higher values of K_2 ($\bar{K}_2/(\beta\,\bar{\mu}) > 1$), are cut-off in the sense that their efficiency is lower than the one of supercritical gusts and decreases with increasing K_2. However their contribution to the sound field is not zero.

Calculations are made here with $c = 13\,cm$ and $M = 0.05$. At $200\,Hz$ ($kc = 0.48$), $|I|$ is a slowly decreasing function of θ, whereas at $1000\,Hz$ ($kc = 2.4$), it increases with θ until 100° and then decreases. The dashed horizontal segment in the right plot shows the level at 160° for small K_2.

Typical directivity patterns in the mid-span plane for parallel and supercritical, oblique gusts are plotted in figures 3 and 4, respectively. The back–scattering has a noticeable effect on the radiation of parallel gusts only at low frequencies, as shown in figure 3. These results agree very well with similar calculations by Howe (2001) in the case of vanishing Mach number for hydroacoustic applications. They correspond to the left, flat part of the plots in figure 2. Figure 4 shows the effect of gust obliqueness on the full solution. Increasing K_2 makes the radiation to beam in an oblique direction upstream,

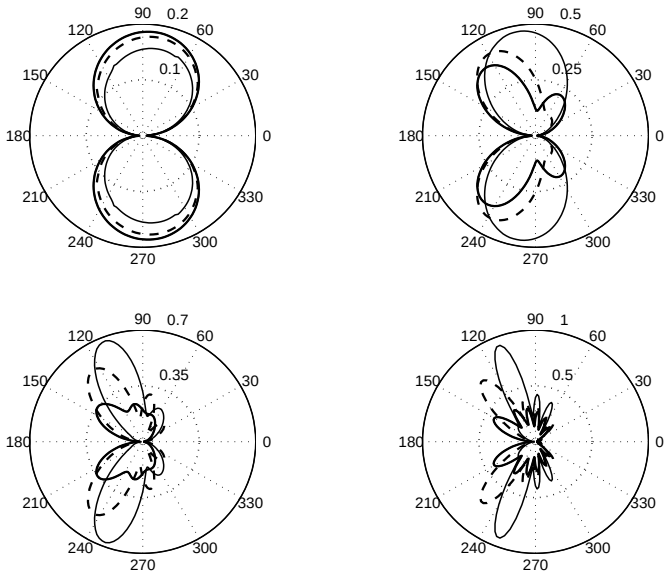

FIGURE 4. Directivity patterns for oblique gusts. From left to right and top to bottom: $kc = 1, 5, 10, 20$. $M = 0.05$, $\bar{K}_2/(\beta\,\bar{\mu}) = 0.05$ —, 0.5 - - , 0.85 — .

more sharply as frequency increases. This effect corresponds to the hump in the radiation profiles of figure 2 for $1000\,Hz$.

A simplified version of the present formulation has been previously reported by Roger & Moreau (2002), for an observer in the mid-span plane. The squared function sinc of formula (2.1) was approximated by a Dirac delta function, which is valid for large aspect ratios. S_{pp}, Φ_{pp} and l_y were measured separately on a mock-up in an anechoic open-jet wind tunnel, in order to evaluate the ratio $S_{pp}/(\Phi_{pp}\,l_y)$. The latter was compared to its theoretical value according to the simplified equation. The measured directivity, integrated over the frequency range attributed to broadband self noise, was also compared to averaged calculations. Sample results are reported in figure 5. The airfoil chord makes a 13° angle with respect to the direction of the mean flow. An encouraging agreement is found, suggesting that the approach is reliable. The remaining discrepancies can be due to either the difficulty of evaluating the convection speed and spanwise coherence length at all frequencies of interest in the experiment, or to the simplification in the analytical model. This motivated the present research.

3. Future plans

The present theory only addresses the question of the transfer function between the hydrodynamic wall pressure and the far field acoustic pressure. The wall pressure statistics defined by Φ_{pp} and l_y and needed as input must be known from either flow measurements or computations. It is not available from RANS calculations that are routinely used by most industrial manufacturers. However, it can be provided by incompressible LES.

The next step, still in progress, is to improve the validation procedure and to use LES results to compute the aforementioned statistical parameters. More precisely, a new experiment with an increased width of the open jet has been designed at Ecole Centrale de Lyon, in order to minimize the installation effects pointed out by Moreau et al (2001).

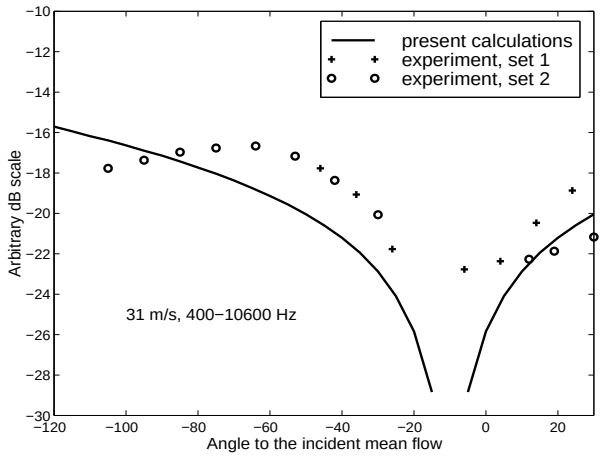

FIGURE 5. Measured versus predicted directivity of the trailing-edge broadband noise due to turbulent boundary layers. Negative angles correspond to an observer facing the suction side.

A simulation of the experimental mean flow has been made with the help of a RANS code. This flow field will be used to provide boundary conditions for an LES, carried out in a smaller domain within the potential core of the jet. First, the LES results will be compared to the measured wall pressure statistics. In the second step, the radiated sound will be calculated using (2.1) and compared to the sound actually measured in the experiment.

4. Appendix

Let Φ be a two-dimensional scalar field solution of the following wave problem:

$$\frac{\partial^2 \Phi}{\partial x^2} + \frac{\partial^2 \Phi}{\partial z^2} + \mu^2 \, \Phi = 0$$
$$\Phi(x,0) = f(x) \qquad x \geq 0$$
$$\frac{\partial \Phi}{\partial z}(x,0) = 0 \qquad x < 0$$

Then for any $x < 0$:

$$\Phi(x,0) = \frac{1}{\pi} \int_0^\infty G(x,\xi,0)\, f(\xi)\, d\xi$$

with:

$$G(x,\xi,0) = \sqrt{\frac{-x}{\xi}}\, \frac{e^{-i\,\mu(\xi - x)}}{\xi - x}$$

This result, known as Schwarzschild's theorem and given in Landahl (1961), leads to mathematical solutions that are equivalent to the ones obtained by Adamczyk (1974) using the Wiener-Hopf technique. Strictly speaking, the theorem holds for half-plane

problems. When applied to an airfoil with finite chord length, it must be used within an iterative procedure involving alternative corrections. According to Amiet (1975), the first two iterations are enough in the problem of the noise generated by the impingement of upstream turbulence on an isolated airfoil. The same is assumed to hold here. The iterations are referred to as main scattering and back-scattering in the text.

REFERENCES

Abramowitz, M. & Stegun, I.A. 1970 *Handbook of Mathematical Functions.* Dover, New York.

Adamczyk, J.J. 1974 *The passage of an infinite swept airfoil through an oblique gust.* NASA CR-2395.

Amiet, R.K. 1975 Acoustic radiation from an airfoil in a turbulent flow. *J. Sound Vib.* **41**, 407–420.

Amiet, R.K. 1976 Noise due to turbulent flow past a trailing edge. *J. Sound Vib.* **47**, 387–393.

Amiet, R.K. 1978 Effect of the incident surface pressure field on noise due to turbulent flow past a trailing edge. *J. Sound Vib.* **57**, 305–306.

Brooks, T.F. & Hodgson, T.H. 1981 Trailing-edge noise prediction from measured surface pressures. *J.Sound Vib.* **78**, 69–117.

Brooks, T.F., Marcolini, M.A. & Pope, D.S. 1989 *Airfoil self-noise and prediction.* NASA RP-1218.

Ffowcs Williams, J.E. & Hawkings, D.L. 1969 Sound generation by turbulence and surfaces in arbitrary motion. *Phil. Trans. Roy. Soc.* **A 264**, 321–342.

Ffowcs Williams, J.E. & Hall, L.H. 1970 Aerodynamic sound generation by turbulent flow in the vicinity of a scattering half-plane. *J. Fluid Mech.* **40**, 657–670.

Howe, M.S. 2001 Edge-source acoustic Green's function for an airfoil of arbitrary chord, with application to trailing-edge noise. *Q. J. Mech. Appl. Math.*, **54**, pp. 139–155.

Landahl, M. 1961 *Unsteady transonic flow.* Pergamon Press, New York.

Moreau, S., Iaccarino, G., Roger, M. & Wang, M. 2001 CFD analysis of flow in an open-jet aeroacoustic experiment. *Annual Research Briefs*, Center for Turbulence Research, NASA Ames/Stanford Univ., 343–351.

Roger, M. & Moreau, S. 2002 Trailing edge noise measurements and prediction for a subsonic loaded fan blade. *AIAA Paper 2022-2460.*

Singer, B.A. 1996 *Turbulent wall-pressure fluctuations: new model for off-axis cross-spectral density.* NASA CR 198297.

Wang, M., & Moin, P. 2000 Computation of trailing-edge flow and noise using large-eddy simulation. *AIAA J.* **38**, 2201–2209.